TABLE 1
Pathological profile of Mac-2BP/CEA expression patterns in cancer tissues with rhDC-SIGN-staining positive specimens ($n = 16$)

Age	Sex	Organ	Digagnosis	pTNM[a]	Stage[a]	Immunostaining[b] Mac-2BP	CEA
59	M	Ascending colon adenocarcinoma	Moderately differentiated	T3N0M0	II A		
62	M	Sigmoid colon adenocarcinoma	Moderately differentiated	T3N2M1	IV	High (18.8%)	High
41	F	Sigmoid colon adenocarcinoma	Well differentiated	T4N2M1	IV		
62	M	Ascending colon adenocarcinoma	Moderately differentiated	T3N0M0	II A		
64	M	Sigmoid colon adenocarcinoma	Moderately differentiated	T3N1M0	III B		
75	F	Rectum adenocarcinoma	Well differentiated	T3N1M0	III B	Low (37.5%)	High
68	M	Sigmoid colon adenocarcinoma	Moderately differentiated	T3N1M0	III B		
65	F	Sigmoid colon adenocarcinoma	Well differentiated	T3N0M0	II A		
56	F	Sigmoid colon adenocarcinoma	Moderately differentiated	T3N2M1	IV		
45	M	Rectum adenocarcinoma	Well differentiated	T3N1M0	III B		
59	M	Sigmoid colon adenocarcinoma	Moderately differentiated	T4N0M0	II B		
62	M	Sigmoid colon adenocarcinoma	Moderately differentiated	T3N0M0	II A	High (31.3%)	Low
57	M	Sigmoid colon adenocarcinoma	Moderately differentiated	T3N0M0	II A		
46	F	Ascending colon adenocarcinoma	Poorly differentiated	T3N2M0	III C		
60	F	Rectum adenocarcinoma	Moderately differentiated	T4N0M0	II B	Low (12.5%)	Low
47	F	Cecum adenocarcinoma	Moderately differentiated	T3N0M0	II A		

[a] AJCC Cancer Staging Manual (6th Edition).
[b] Tissue specimens were stained with anti-CEA mAb and anti-Mac-2BP followed by Alexa Fluor-conjugated secondary Abs.

glycans on human colorectal carcinoma cells, suggesting that increased expression of DC-SIGN ligands on colorectal cancer cells in addition to altered glycosylation results in recognition by DC-SIGN and that further fucosylation of polylactosamine glycans and formation of Le epitopes on Mac-2BP during cancer progression may be important for induction of the interaction between DC-SIGN and Mac-2BP. In addition, we also found that the expression levels of Le epitopes were positively correlated with the staining levels with rhDC-SIGN in 30 colorectal carcinoma cell lines, including LoVo, LS513, LS174T, SNU1197, etc. (data not shown).

CEA is one of the most widely used tumor markers for gastrointestinal cancer such as colorectal carcinomas. It has been pointed out that the change in distribution of CEA from apical into basolateral and stromal areas in malignant colorectal cancer tissues could be a cause of its entry into the blood and elevation of the serum CEA levels (14, 16). However, the sensitivity and specificity of CEA are considered to be low, particularly for early stages of the disease such as Dukes A or B stages (26). We showed here that the distribution of Mac-2BP was more basolateral than that of CEA and that expression of Mac-2BP in primary colon adenocarcinoma tissues was increased compared with in proximal normal tissues and obtained various staining patterns for Mac-2BP such as luminal staining and punctate staining on the apical and basolateral faces (Fig. 7*B*). In addition, we observed here that DC-SIGN greatly associated with not only CEA but also Mac-2BP on the apical face of cancer epithelia and that DC-SIGN retained responsiveness to Mac-2BP in more basolateral areas. Because basolateral expression of Mac-2BP has been reported to be more prevalent in early stage Dukes A tumors than in advanced ones (12), DC-SIGN may preferably recognize early stage colorectal carcinoma cells through Mac-2BP. Therefore, similarly to that of CEA, aberrant expression of Mac-2BP and its polar breakdown in cancer tissues may allow its entry into blood vessels. Furthermore, it is also interesting that the type of Mac-2BP secreted by several colorectal carcinoma cells had DC-SIGN-detectable glycan structures, whereas we did not detect any binding of DC-SIGN to serum Mac-2BP from healthy donors (data not shown), suggesting that DC-SIGN can qualitatively distinguish colorectal carcinoma-derived Mac-2BP from serum Mac-2BP in normal and cancer patients.

Recent evidence indicates that dendritic cell-associated DC-SIGN may have functions in both the induction of tolerance to self-antigens and the recognition of pathogens, respectively. A variety of cytokines, including IL-6, IL-10, and macrophage colony-stimulating factor (M-CSF), have been shown to affect the maturation of DCs from $CD34^+$ precursors and from MoDCs *in vitro* (27, 28). Failure of the immune system to provide protection against tumor cells is an important immunological problem. It is now evident that inadequate functioning of the host immune system is one of the main mechanisms by which tumors escape from immune control, as well as an important factor that limits the success of cancer immunotherapy. In recent years, it has become increasingly clear that defects in DCs play a crucial role in non-responsiveness to tumors (29). Here, we showed that DC-SIGN-dependent cellular interactions between immature MoDCs and colorectal carcinoma cells significantly inhibited MoDC functional maturation, suggesting that, similar to CEA, Mac-2BP bearing colorectal tumor-associated Le glycans may provide a tolerogenic microenvironment for colorectal carcinoma cells through interactions with DC-SIGN. These findings also imply that the glycosylation-dependent cellular interactions may result in suppression of DC functions, possibly through immunosuppressive cytokines such as IL-6 and IL-10, and that production of these immunosuppressive factors in DC tumor coculture supernatants may be one of the mechanisms by which tumors evade immunosurveillance.

Recently, the intracellular signaling mechanisms of DC-SIGN were elucidated (30–32). DC-SIGN constitutively associates with a signalosome complex consisting of scaffold protein LSP1 and mediates cross-talk with Toll-like receptor signaling, which results in modulation of Toll-like receptor-induced cytokine responses. Indeed, interaction of foreign pathogens such as *M. tuberculosis* leads to up-regulation of LPS-induced IL-10 and suppresses MoDC maturation (33). Therefore, the MoDC maturation as a consequence of DC-SIGN interacting with Le glycans of cancer cells may also be mediated through a series of LSP1-associated intracellular signaling pathway. MoDCs, following sensitization with CEA-derived peptides *ex vivo*, are now utilized as a tool for the clinical applications of tumor immunotherapies. As the immunogenicities of peptide vaccines vary among patients who exhibit different immune responsiveness, which is defined by means of human leukocyte antigen (HLA) types, etc., appropriate selection of antigens is needed individually to obtain adequate therapeutic benefit. In this context, colorectal carcinoma-derived Mac-2BP, similar to CEA, might become a candidate new cancer vaccine. Canceling of tumor-escaping mechanisms, such as DC-SIGN-mediated MoDC dysfunction, by combination of therapeutic agents that target intracellular signaling molecules (*e.g.* LSP1) may be a critical step for maintaining the effective tumor-immunogenicity in the future.

In conclusion, based on the distinct expression patterns of Mac-2BP and CEA together with the DC-SIGN recognition model presented here, colorectal cancer patients could be divided into $Mac\text{-}2BP^{high}/CEA^{high}$, $Mac\text{-}2BP^{low}/CEA^{high}$,

Mac-2BP^{high}/CEA^{low}, and Mac-2BP^{low}/CEA^{low} groups. The establishment of a model of the DC-SIGN-Mac-2BP/CEA interaction is a valuable step toward elucidation of the physiological function and molecular mechanism and provides a knowledge-based approach for the clinical applications of cancer immunotherapies and novel diagnoses. For this purpose, identification of the DC-SIGN-Mac-2BP/CEA model that breaks immunotolerance to Mac-2BP/CEA and induces cancer immunosurveillance failure both *in vitro* and *in vivo* is therefore a major goal for therapeutic applications in the future.

Acknowledgment—We thank Tomoko Tominaga for secretarial assistance.

REFERENCES

1. Banchereau, J., Briere, F., Caux, C., Davoust, J., Lebecque, S., Liu, Y. J., Pulendran, B., and Palucka, K. (2000) *Annu. Rev. Immunol.* **18,** 767–811
2. Lanzavecchia, A., and Sallusto, F. (2001) *Cell* **106,** 263–266
3. Geijtenbeek, T. B., van Vliet, S. J., Engering, A., 't Hart, B. A., and van Kooyk, Y. (2004) *Annu. Rev. Immunol.* **22,** 33–54
4. van Vliet, S. J., den Dunnen, J., Gringhuis, S. I., Geijtenbeek, T. B., and van Kooyk, Y. (2007) *Curr. Opin. Immunol.* **19,** 435–440
5. van Kooyk, Y., and Rabinovich, G. A. (2008) *Nat. Immunol.* **9,** 593–601
6. Geijtenbeek, T. B., Kwon, D. S., Torensma, R., van Vliet, S. J., van Duijnhoven, G. C., Middel, J., Cornelissen, I. L., Nottet, H. S., KewalRamani, V. N., Littman, D. R., Figdor, C. G., and van Kooyk, Y. (2000) *Cell* **100,** 587–597
7. Geijtenbeek, T. B., Torensma, R., van Vliet, S. J., van Duijnhoven, G. C., Adema, G. J., van Kooyk, Y., and Figdor, C. G. (2000) *Cell* **100,** 575–585
8. van Liempt, E., Bank, C. M., Mehta, P., Garciá-Vallejo, J. J., Kawar, Z. S., Geyer, R., Alvarez, R. A., Cummings, R. D., Kooyk, Y., and van Die, I. (2006) *FEBS Lett.* **580,** 6123–6131
9. van Gisbergen, K. P., Aarnoudse, C. A., Meijer, G. A., Geijtenbeek, T. B., and van Kooyk, Y. (2005) *Cancer Res.* **65,** 5935–5944
10. Nonaka, M., Ma, B. Y., Murai, R., Nakamura, N., Baba, M., Kawasaki, N., Hodohara, K., Asano, S., and Kawasaki, T. (2008) *J. Immunol.* **180,** 3347–3356
11. Grassadonia, A., Tinari, N., Iurisci, I., Piccolo, E., Cumashi, A., Innominato, P., D'Egidio, M., Natoli, C., Piantelli, M., and Iacobelli, S. (2004) *Glycoconj. J.* **19,** 551–556
12. Ulmer, T. A., Keeler, V., Loh, L., Chibbar, R., Torlakovic, E., André, S., Gabius, H. J., and Laferté, S. (2006) *J. Cell Biochem.* **98,** 1351–1366
13. Midiri, G., Amanti, C., Benedetti, M., Campisi, C., Santeusanio, G., Castagna, G., Peronace, L., Di Tondo, U., Di Paola, M., and Pascal, R. R. (1985) *Cancer* **55,** 2624–2629
14. Hamada, Y., Yamamura, M., Hioki, K., Yamamoto, M., Nagura, H., and Watanabe, K. (1985) *Cancer* **55,** 136–141
15. Shi, Z. R., Tsao, D., and Kim, Y. S. (1983) *Cancer Res.* **43,** 4045–4049
16. Ahnen, D. J., Nakane, P. K., and Brown, W. R. (1982) *Cancer* **49,** 2077–2090
17. Nittka, S., Böhm, C., Zentgraf, H., and Neumaier, M. (2008) *Oncogene* **27,** 3721–3728
18. Shively, J. E. (2004) *Oncogene* **23,** 9303–9305
19. Nittka, S., Günther, J., Ebisch, C., Erbersdobler, A., and Neumaier, M. (2004) *Oncogene* **23,** 9306–9313
20. Seelentag, W. K., Li, W. P., Schmitz, S. F., Metzger, U., Aeberhard, P., Heitz, P. U., and Roth, J. (1998) *Cancer Res.* **58,** 5559–5564
21. Dennis, J. W., Laferté, S., Waghorne, C., Breitman, M. L., and Kerbel, R. S. (1987) *Science* **236,** 582–585
22. Laferté, S., and Loh, L. C. (1992) *Biochem. J.* **283,** 193–201
23. Fernandes, B., Sagman, U., Auger, M., Demetrio, M., and Dennis, J. W. (1991) *Cancer Res.* **51,** 718–723
24. Appelmelk, B. J., van Die, I., van Vliet, S. J., Vandenbroucke-Grauls, C. M., Geijtenbeek, T. B., and van Kooyk, Y. (2003) *J. Immunol.* **170,** 1635–1639
25. Guo, Y., Feinberg, H., Conroy, E., Mitchell, D. A., Alvarez, R., Blixt, O., Taylor, M. E., Weis, W. I., and Drickamer, K. (2004) *Nat. Struct. Mol. Biol.* **11,** 591–598
26. Duffy, M. J. (2001) *Clin. Chem.* **47,** 624–630
27. Menetrier-Caux, C., Montmain, G., Dieu, M. C., Bain, C., Favrot, M. C., Caux, C., and Blay, J. Y. (1998) *Blood* **92,** 4778–4791
28. Kiertscher, S. M., Luo, J., Dubinett, S. M., and Roth, M. D. (2000) *J. Immunol.* **164,** 1269–1276
29. Gabrilovich, D. (2004) *Nat. Rev. Immunol.* **4,** 941–952
30. Gringhuis, S. I., den Dunnen, J., Litjens, M., van Het Hof, B., van Kooyk, Y., and Geijtenbeek, T. B. (2007) *Immunity* **26,** 605–616
31. Gringhuis, S. I., van der Vlist, M., van den Berg, L. M., den Dunnen, J., Litjens, M., and Geijtenbeek, T. B. (2010) *Nat. Immunol.* **11,** 419–426
32. Gringhuis, S. I., den Dunnen, J., Litjens, M., van der Vlist, M., and Geijtenbeek, T. B. (2009) *Nat. Immunol.* **10,** 1081–1088
33. Geijtenbeek, T. B., Van Vliet, S. J., Koppel, E. A., Sanchez-Hernandez, M., Vandenbroucke-Grauls, C. M., Appelmelk, B., and Van Kooyk, Y. (2003) *J. Exp. Med.* **197,** 7–17

Glycobiology vol. 22 no. 1 pp. 84–95, 2012
doi:10.1093/glycob/cwr107
Advance Access publication on August 10, 2011

Role of interaction of mannan-binding protein with meprins at the initial step of complement activation in ischemia/reperfusion injury to mouse kidney

Makoto Hirano[2,3,4,8], Bruce Y Ma[3,5,6,9], Nobuko Kawasaki[3], Shogo Oka[7], and Toshisuke Kawasaki[1,3]

[2]Department of Biological Chemistry, Graduate School of Pharmaceutical Sciences, Kyoto University, Kyoto 606-8501, Japan; [3]Research Center for Glycobiotechnology, Ritsumeikan University, Shiga 525-0058, Japan; [4]Institute of Glycoscience, Tokai University, Kanagawa 259-1292, Japan; [5]Department of Computer Science and Systems Engineering, Muroran Institute of Technology, Hokkaido 050-8585, Japan; [6]School of Pharmaceutical Engineering and Life Science, Changzhou University, Jiangsu 213164, People's Republic of China; and [7]School of Health Sciences, Faculty of Medicine, Kyoto University, Kyoto 606-8501, Japan

Received on May 13, 2011; revised on July 20, 2011; accepted on July 29, 2011

Ischemia/reperfusion (I/R) is an important cause of acute renal failure. Recent studies have shown that the complement system mediated by the mannan-binding protein (MBP), which is a C-type serum lectin recognizing mannose, fucose and *N*-acetylglucosamine residues, plays a critical role in the pathogenesis of ischemic acute renal failure. MBP causes complement activation through the MBP lectin pathway and a resulting complement component, C3b, is accumulated on the brush borders of kidney proximal tubules in a renal I/R-operated mouse kidney. However, the initial step of the complement activation has not been studied extensively. We previously identified both meprins α and β, highly glycosylated zinc metalloproteases, localized on kidney proximal tubules as endogenous MBP ligands. In the present study, we demonstrated that serum-type MBP (S-MBP) and C3b were co-localized with meprins on both the cortex and the medulla in the renal I/R-operated mouse kidney. S-MBP was indicated to interact with meprins in vivo in the I/R-operated mouse kidney and was shown to initiate the complement activation through the interaction with meprins in vitro. Taken together, the present study strongly suggested that the binding of S-MBP to meprins triggers the complement activation through the lectin pathway and may cause the acute renal failure due to I/R on kidney transplantation and hemorrhagic shock.

Keywords: cute renal failure / C3b / complement activation / C-type lectin / lectin pathway

Introduction

Ischemia/reperfusion (I/R) is an important cause of acute renal failure. Various clinical conditions such as intravascular volume depletion and hypotension can result in a reduction in renal blood flow, which leads to ischemic acute renal failure (Thadhani et al. 1996). The pathophysiology of renal I/R injury is complicated, but recent studies indicated that activation of complement through the lectin pathway plays a critical role in the pathogenesis of ischemic acute renal failure (de Vries et al. 2004). In the lectin pathway, mannan-binding protein (MBP), also known as mannan-binding lectin (MBL), binds to ligand carbohydrates on the cell surface and activates MBP-associated serine proteases (MASPs). Subsequently, activated MASPs cleave complement components C2 and C4 to yield C3 convertase, which can lead MBP-bound cells to necrosis. However, it is not clear what molecules interact with MBP at the initial stage of the complement activation in renal I/R. Although immunoglobulin M (IgM) triggers the lectin pathway in mesenteric I/R (Zhang et al. 2006), renal I/R does not induce IgM deposition (Park et al. 2002).

MBP recognizes D-mannose, L-fucose and *N*-acetyl-D-glucosamine residues Ca^{2+}-dependently. Human have only one MBP gene, whereas rodents have two MBPs encoded by separate genes, one is serum-type MBP termed S-MBP, MBL-1 or MBL-A and the other is liver-type MBP termed L-MBP, MBL-2 or MBL-C. Both MBPs are mostly synthesized by hepatocytes and secreted into the serum. However, a small amount of S-MBP, but not L-MBP, is synthesized in the mouse (Wagner et al. 2003) and rat (Morio et al. 1997) kidneys. Both mouse S- and L-MBPs can mediate the activation of C4 (Hansen et al. 2000; Liu et al. 2001), although they recognize different bacterial pathogens (Phaneuf et al. 2007).

We previously reported that endogenous MBP ligands are highly expressed on the brush borders of proximal tubules of the normal mouse kidney and the ligands were identified as

[1]To whom correspondence should be addressed: Tel: +81-77-561-3444; Fax: +81-77-561-3444; e-mail: tkawasak@fc.ritsumei.ac.jp
[8]Present address: Institute of Glycoscience, Tokai University, Kanagawa 259-1292, Japan.
[9]Present address: School of Pharmaceutical Engineering and Life Science, Changzhou University, Jiangsu 213164, People's Republic of China.

meprins α and β (Hirano et al. 2005). Meprins are highly glycosylated zinc metalloproteases abundantly expressed in kidney and intestinal epithelial cells, comprising ~5% of the total brush border membrane proteins in the rodent kidneys (Bond and Beynon 1986). Mouse meprin A (EC 3.4.24.18) is a homo-oligomer of α subunits or a hetero-oligomer of α and β subunits (Marchand et al. 1994). Mouse meprin B (EC 3.4.24.63) is a homo-oligomer of β subunits (Gorbea et al. 1993). Meprin α and β subunits form a disulfide-linked dimer and higher-order oligomers through non-covalent interactions (Gorbea et al. 1991). Meprin α has a tendency to form huge complexes with a molecular mass of 1–8 MDa, which comprise 10–100 subunits (Ishmael et al. 2001).

In the present study, we studied the functional role of interaction of MBP with meprins in the I/R-operated mouse kidney, because of the facts that meprins are endogenous ligands for MBP, abundantly expressed in the kidneys and self-aggregate into high-molecular mass complexes that is an important requirement for complement activation to occur. We demonstrated that recombinant mouse S-MBP, but not L-MBP, significantly activated complement by binding to meprins in vitro. Immunohistochemical analysis indicated that S-MBP partially co-localized with meprins in vivo. Additionally, the results of immunoprecipitation (IP) of meprins or S-MBP and in situ proximity ligation assay (PLA; Söderberg et al. 2006) of the renal I/R-operated mouse kidney indicated strongly the functional interaction of S-MBP with meprins in vivo. Protein quantification by western blotting indicated that the amount of S-MBP increased several-fold in the I/R-operated mouse kidney, whereas real-time polymerase chain reaction (PCR) revealed that the amount of S-MBP messenger RNA (mRNA) did not increase in the I/R-operated kidney. These results suggested the possibility that S-MBP increment in the I/R-operated kidney may be due to outflow from the blood circulation rather than the induction of S-MBP mRNA expression in the kidney. Thus, our findings suggested that S-MBP mostly derived from serum interact with meprins and initiates the complement activation through the lectin pathway in renal I/R injury.

Results

Preparation of I/R-operated mice

The experimental renal I/R-operated mouse has been established as a model of acute renal failure. Mice subjected to renal I/R operation exhibited the renal deposition of MBP and complement components and induction of tubular necrosis through the formation of membrane attack complexes (de Vries et al. 2004). We found a high-level expression of endogenous ligands for MBP in the epithelial cells of the kidney proximal tubules and subsequently identified metalloproteases, meprins α and β (meprins) as the predominant MBP ligands (Hirano et al. 2005). Based on this background, we hypothesized that the interaction of MBP with meprins may trigger the activation of complement, resulting in tubular necrosis. In order to test this, we investigated the localization of MBP, meprins and complement component C3b, an activated form of C3, and the protein levels of MBP and meprins, and also the mRNA expression levels of these proteins in the renal I/R-operated mouse kidney. Ischemia was induced by bilateral renal artery clamping and blood urea nitrogen (BUN) was monitored as an index of renal injury. Table I shows BUN level time courses in sham- and I/R-operated mice ($n = 4$). The starting point (0 h) indicates the time when the clamps were removed from the renal arteries. BUN increased gradually during reperfusion and reached at ~3- and 6-fold higher values after 6 and 24 h reperfusion in I/R-operated mice, respectively. We used I/R-operated mice that had reperfused for 6 h in the following experiments.

The localization of meprins, S-MBP and complement C3b in the I/R-operated mouse kidney

Immunohistochemical analysis using a laser confocal microscope indicated marked changes in the distribution of meprin β, S-MBP and C3b in association with I/R operation (Figures 1 and 2). Thus, meprin β was strictly localized in the cortex in the sham-operated mouse kidney (Figure 1A), whereas in the I/R-operated kidney, meprin β was expressed not only in the cortex but also in the medulla significantly (Figure 1G). To the contrary, S-MBP was not detected in the sham-operated kidney (Figure 1B). In the clear contrast to this, in the I/R-operated mouse kidney, S-MBP was massively accumulated in the cortex and, in addition, weak staining was detected in some parts of the medulla (Figure 1H). In higher-magnification views, meprin β in the cortex of the sham-operated mouse kidney was selectively localized on the apical surface of the proximal tubules (Figure 1E). On the other hand, in the I/R-operated mouse kidney, a significant portion of meprin β was detected on the base of the brush border, although there were slight morphological changes in the I/R-operated mouse kidney (Figure 1K). Overlay images indicated that S-MBP was co-localized with meprin β on the base of the brush border of the proximal tubules (Figure 1K) and the medulla (Figure 1L).

Figure 2 indicates that similar changes occurred in the distribution of a complement component, C3b, in association with I/R operation. C3b was hardly detected in the sham-operated mouse kidney (Figure 2B). In the clear contrast, in the I/R-operated mouse kidney, C3b was heavily

Table I. Determination of BUN (mg/dL) before and after renal I/R operation

Time (h)	−0.67	0	1	3	6	12	24
Sham	24 ± 4.3	24 ± 4.1	27 ± 4.4	25 ± 2.8	28 ± 3.0	24 ± 8.0	20 ± 2.8
I/R	25 ± 3.0	32 ± 3.0	38 ± 3.9	56 ± 7.8	73 ± 14.5	124 ± 22.7	160 ± 45.0

Renal function before ischemia (−0.67) and 0, 1, 3, 6, 12 and 24 h after 40 min ischemia. The data are expressed as mean ± SD ($n = 4$).

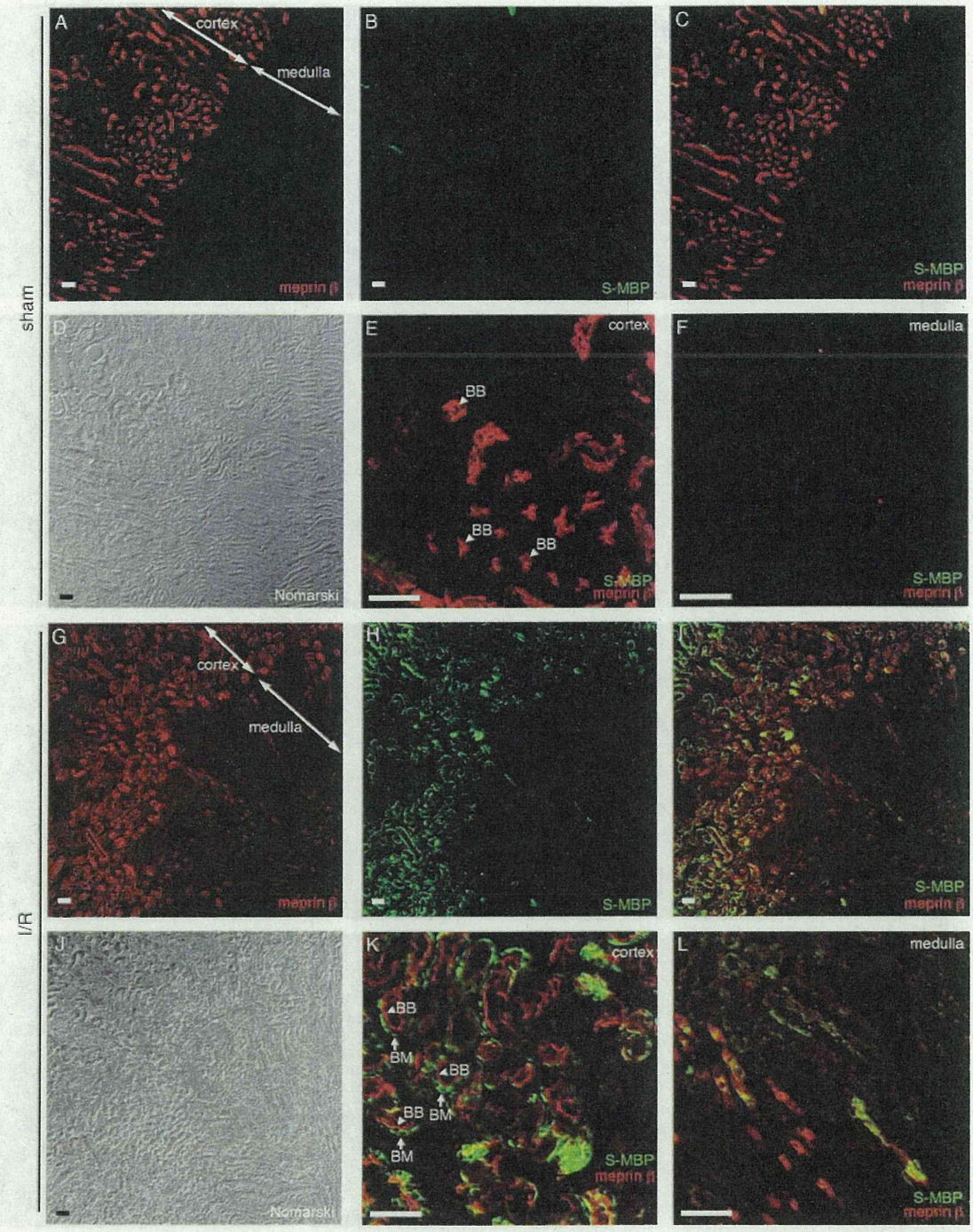

Fig. 1. Localization of S-MBP and meprin β in the renal I/R-operated mouse kidney. Representative kidney paraffin sections (10 μm) were harvested following renal I/R (reperfused for 6 h) and stained with both anti-meprin β and anti-S-MBP antibodies. Cortical and medullary regions are indicated with double arrows in (A) and (G). (**A**) Meprin β (red) was localized strictly in the cortex. (**G**) Meprin β was localized not only in the cortex but also in the medulla. (**B**) S-MBP (green) was not detected. (**H**) S-MBP massively deposited in the cortex and, in addition, S-MBP was weakly detected in the medulla. (**C**) Overlay image of (A) with (B). (**I**) Overlay image of (G) with (H) shows that S-MBP is co-localized with meprin β mostly in the cortex. (**D** and **J**) Nomarski micrographs of (A)–(C) and (G) and (H), respectively. (**E**, **K**, **F** and **L**) Higher-magnification views of cortical regions of (C) and (I) and medullary regions of (C) and (I), respectively. Arrowheads and arrows indicate the brush border membranes (BB) and the basolateral membranes (BM) of the proximal tubules, respectively. (**E**) Meprin β was strictly localized on the brush border membrane of the proximal tubules, but S-MBP was not detected. (**K**) The brush border membranes of the proximal tubules changed morphologically. S-MBP was partially co-localized with meprin β on the base of the brush border membrane of the proximal tubules. (**F**) Neither S-MBP nor meprin β were detected. (**L**) S-MBP was partially co-localized with meprin β. Bars, 100 μm.

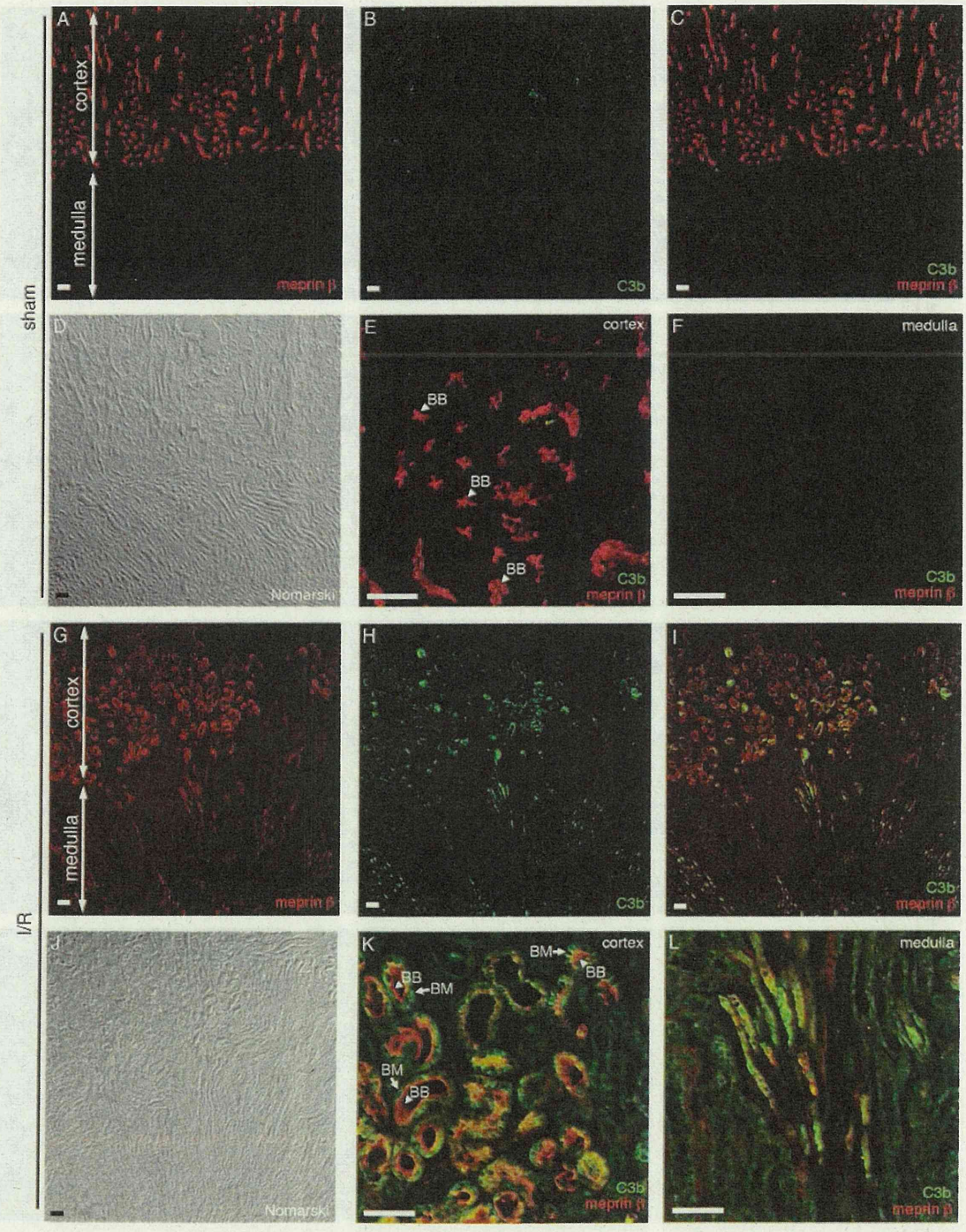

Fig. 2. Localization of C3b and meprin β in the renal I/R-operated mouse kidney. Representative kidney paraffin sections (10 μm) were harvested following renal I/R (reperfused for 6 h) and stained with both anti-meprin β and anti-C3b antibodies. Cortical and medullary regions are indicated with double arrows in (A) and (G). (**A**) Anti-meprin β (red) strictly stained the cortex. (**G**) Anti-meprin β stained not only the cortex but also the medulla. (**B**) C3b (green) was not detected. (**H**) C3b was detected abundantly in the cortex and weakly in the medulla. (**C**) Overlay image of (A) with (B). (**I**) Overlay image of (G) with (H) shows that C3b is co-localized with meprin β mostly in the cortex. (**D** and **J**) Nomarski microphotographs of (A)–(C) and (G) and (H), respectively. (**E**, **K**, **F** and **L**) Higher-magnification views of cortical regions of (C) and (I) and medullary regions of (C) and (I), respectively. Arrowheads and arrows indicate the brush border membranes (BB) and the basolateral membranes (BM) of the proximal tubules, respectively. (**E**) Meprin β was strictly localized on the brush border membrane of the proximal tubules. No signals of C3b were detected. (**K**) C3b was co-localized with meprin β mostly on the base of the brush border membrane of the proximal tubules. (**F**) Neither C3b nor meprin β were detected. (**L**) C3b was partially co-localized with meprin β. Bars, 100 μm.

accumulated in the proximal tubular cells (Figure 2H). C3b was co-localized with meprin β for the most part on the brush border membranes of the proximal tubules (Figure 2K) and in the medulla (Figure 2L).

The immunohistochemical data presented in Figures 1 and 2 indicate clearly that meprin β is an intrinsic component of the normal brush border membranes of the proximal tubules in the cortex, while S-MBP and C3b are not the normal components in this part of the mouse kidney and they appeared only after I/R operation. In addition, the strict localization of meprin β in the cortex was partially abolished and meprin β appeared in the medulla to some extent. Interestingly, S-MBP and C3b, which appeared in the kidney after I/R operation, are co-localized with meprin β on the base of the brush border of the proximal tubules, suggesting a possibility of a functional contact between meprin β and S-MBP. Furthermore, meprin α was co-localized with both S-MBP and C3b in the same manner as meprin β, and L-MBP could not be detected in the kidney (data not shown).

In situ interaction of S-MBP with meprins in the I/R-operated mouse kidney

In order to examine the molecular interaction of S-MBP with meprins in vivo, co-IP experiments were carried out. Small pieces of sham- and I/R-operated mouse kidney cortexes ($n = 3$) were subjected to chemical cross-linking with dithiobis (succinimidylpropionate) (DSP), followed by homogenization and extraction with Nonidet P-40 (NP-40). NP-40 extracts were incubated with antibody specific to S-MBP or meprins, and the immunoprecipitates were analyzed by western blotting after sodium dodecyl sulfate (SDS)–polyacrylamide gel electrophoresis (PAGE). As shown in Figure 3A, multiple S-MBP bands, which probably represent monomer, dimer and trimer of the structural unit of S-MBP, were detected in co-immunoprecipitates with either meprin α (left panel) or meprin β (right panel) as indicated by arrowheads. The estimated molecular masses of trimer, dimer and monomer of the structural unit of S-MBP were 220, 160 and 117 kDa, respectively; in contrast, theoretical molecular masses of trimer, dimer and monomer of the structural unit were ~270, 180 and 90 kDa, respectively. Thus, higher oligomers are estimated to be smaller than their respective theoretical values under non-reducing conditions tested. The reasons for these discrepancies are not clear at the moment but this might be due to incomplete denaturation of higher oligomers because of the presence of intrachain disulfide bonds within the monomeric subunit of S-MBP, interchain disulfide bonds between the subunit components of S-MBP and also newly formed cross-links by DSP treatment. Reversely, as shown in Figure 3B, multiple bands of meprins α and β, probably representing, homo- or heterodimers and trimers of meprins α (left panel) and β (right panel), respectively, were detected in co-immunoprecipitates with S-MBP as indicated by arrowheads. In these two sets of experiments, protein levels of S-MBP and meprins co-immunoprecipitated with meprins and S-MBP, respectively, from the I/R-operated mouse kidney were significantly higher than those from the sham-operated mouse kidney. Furthermore, in the case of the I/R-operated mouse kidney, several larger molecular size bands (indicated by arrows), which probably correspond to DSP cross-linked complexes of S-MBP and meprin β, were observed. It should be noted that the protein bands of meprins and S-MBP, which were immunoprecipitated directly with the same amounts of the respective specific antibodies, were essentially the same either from the I/R-operated mouse kidneys or from the sham-operated mouse kidneys under the conditions examined (data not shown). Taken together, these results indicated that S-MBP and meprins were located close enough to interact with each other in the I/R-operated mouse kidney.

This interaction of S-MBP with meprins in the I/R-operated mouse kidney was further confirmed by in situ PLA of the kidney section. The requirement for dual recombination of pairs of antibodies in combination with very potent signal amplification makes in situ PLA, a powerful tool for identifying numerous interacting proteins and also their subcellular distributions (Söderberg et al. 2006). As shown in the diagram in Figure 3C, when S-MBP and meprins are within 40 nm in proximity, oligonucleotides (plus and minus chains) conjugated with secondary antibodies will hybridize each other to form a circular oligonucleotide. A DNA polymerase will generate a repeated sequence product extended from the circular oligonucleotide as a template. The repeated sequence product will be hybridized to Tex613 fluorophore-labeled oligonucleotide probes. The fluorescent signals indicate the proximity of S-MBP and meprins in situ. As shown in Figure 3D, Tex613 fluorescent signals, which indicate in situ proximity of S-MBP and meprin β, were observed on the base of the brush border of the proximal tubular epithelial cells of the I/R-operated mouse kidney, whereas essentially no signal was detected in the sham-operated mouse kidney. Similarly, essentially no signal was detected in the negative controls that had undergone staining without either primary antibody (neither anti-S-MBP nor anti-meprin β) or without either of the paired primary antibodies (either anti-S-MBP or anti-meprin β) (data not shown). In addition, a signal reflecting the proximity of S-MBP and meprin α was observed in the same manner as for meprin β (data not shown). These results indicate convincingly that S-MBP interacts with meprins in vivo to form macromolecular complexes, which may induce the activation of complement in the I/R-operated mouse kidney.

The activation of complement through the interaction of S-MBP with meprins in vitro

In order to determine whether the interaction of MBP with meprins activates complement, we developed an enzyme-linked immunosorbent assay (ELISA) system involving purified meprins from the normal mouse kidneys and recombinant mouse MBPs. In this assay system, microtiter wells were coated with biotinylated meprins or IgM Fc and filled with or without recombinant mouse S- or L-MBP. Subsequently, human C4 was added to the wells and then the deposited C4b was detected by adding horseradish peroxidase (HRP)-conjugated anti-human C4 monoclonal antibody (mAb). IgM Fc was used as a positive control, since IgM Fc is known to be a good ligand for MBP due to high-mannose-type *N*-glycans attached to the molecule. As shown in Figure 4, meprins demonstrated a remarkable

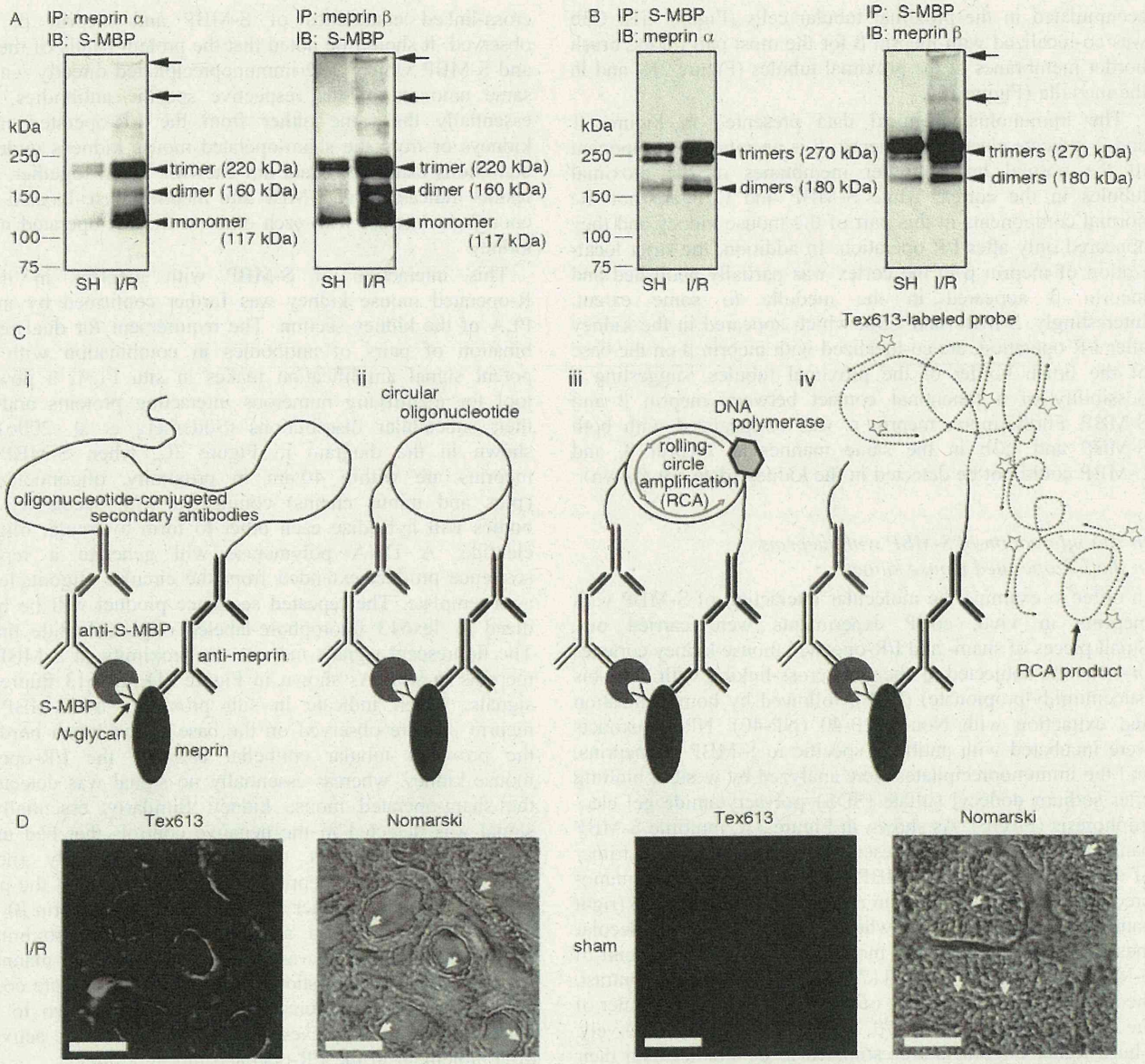

Fig. 3. Interaction of S-MBP with meprins in the I/R-operated mouse kidney. (**A** and **B**) Interaction of S-MBP with meprins after DSP cross-linking. Small pieces of an I/R- and a sham (SH)-operated mouse kidney cortex were cross-linked with 10 mM DSP, and then NP-40 extracts of homogenate were treated with anti-meprin α, anti-meprin β or S-MBP antibody (IP). The complexes were precipitated with Protein G-Sepharose 4B, eluted with SDS–PAGE sample buffer and resolved on a 5–20% Tris–HCl polyacrylamide gradient gel under non-reducing conditions, followed by transfer to nitrocellulose membranes. The immunoblots (IB) were probed with antibodies to S-MBP (A) or meprins (B). The arrows indicate the cross-linked complexes, which consist of S-MBP and meprin α or β. The arrowheads indicate the oligomers of the structural unit of S-MBP and the homo- or hetro-oligomers of meprins on (A) and (B), respectively. (**C**) Diagrams of the principle of in situ PLA. (i) S-MBP and meprin are recognized by specific primary antibodies. Subsequently, the primary antibodies are probed with respective secondary antibodies conjugated with an oligonucleotide (plus or minus chain). (ii) When S-MBP and meprin are within 40 nm in proximity, oligonucleotides will hybridize each other to form a circular oligonucleotide. (iii) A DNA polymerase will generate an RCA product. (iv) The RCA product will be hybridized to a Tex613 fluorophore-labeled probe. The fluorescent signals indicate the proximity of S-MBP and meprin in situ. (**D**) Interaction of S-MBP with meprin β on in situ proximity analysis. Representative kidney paraffin sections (10 μm) were harvested following renal I/R (reperfused for 6 h). The I/R-operated (left two) and the sham-operated (right two) mouse kidneys were used for the in situ proximity assay, as described in *Materials and methods*. The Tex613 signals indicate in situ interaction between S-MBP and meprin β. Arrows indicate the apical surface of the proximal tubules. Bars, 25 μm.

complement activating ability in the presence of S-MBP, which was 4–5-fold higher than that of IgM Fc, this being consistent with the histochemical co-localization of C3b with S-MBP and meprins (Figures 1 and 2). On the other hand, L-MBP did not show essentially any activity under the conditions examined.

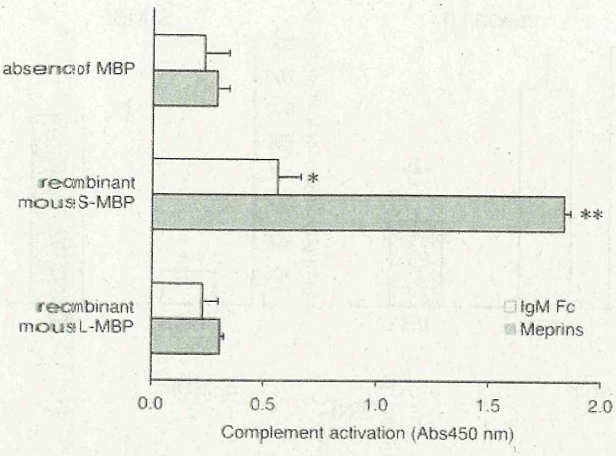

Fig. 4. Activation of complement through the lectin pathway by the interaction of S-MBP and meprins. Each microtiter well was coated with 1.0 μg of biotinylated meprin or IgM Fc and filled with 1.5 μg of recombinant mouse S- or L-MBP. Subsequently, 0.2 μg of human C4 was added to each well and then the deposited C4b was detected by adding HRP-conjugated anti-human C4 mAb, as described in *Materials and methods*. IgM Fc was used as a positive control. Neither S- nor L-MBP was included in the negative controls. The horizontal axis indicates the intensity of C4b deposition in the wells read at 450 nm. All experiments were performed in triplicate and were repeated three times. The data are expressed as means with SD. $*P < 0.05$ and $**P < 0.01$.

Determination of meprins and S-MBP in the I/R-operated mouse kidney

To examine the quantitative changes of meprins and S-MBP in the kidneys in association with I/R operation, we performed western blot analysis of SDS lysates of renal cortex homogenates. Consistent with the result of histochemical studies (see Figure 1), the density of the S-MBP band in the I/R-operated mouse kidney dramatically increased. In contrast, the densities of the meprin α and β bands decreased significantly in the I/R-operated mouse kidney (Figure 5A). Protein was determined as band density, after normalization to the density of β-tubulin (Figure 5B–D). S-MBP increased by almost 5-fold (Figure 5D), whereas both meprins α and β decreased by ~60% (Figure 5B and C). The reason why meprins α and β decreased significantly with I/R operation is not currently clear but it is probably due to partial disorganization of the brush border membrane of the proximal tubular cells, as shown in Figures 1 and 2, where the brush borders seem to be detached from the apical surface on the proximal tubules in the I/R-operated mouse kidney.

The expression of mRNAs of meprins and S-MBP in the I/R-operated mouse kidney

Since S-MBP is expressed in the glomerular mesangial cells of the rat and mouse kidneys (Morio et al. 1997; Wagner et al. 2003), it is possible that I/R operation induces S-MBP expression and increases the quantity of S-MBP protein in the kidney. In order to confirm this, total RNA samples extracted from sham- and I/R-operated mouse kidney cortexes ($n = 6$) were subjected to real-time PCR analysis with target-specific primers. The expression of each mRNA was normalized as to that of glyceraldehyde-3-phosphate dehydrogenase (GAPDH). Figure 5G shows that I/R operation did not increase significantly the expression of S-MBP mRNA. On the other hand, mRNA expression of meprins α and β in the I/R-operated mouse kidneys decreased by 30% (Figure 5E) and 60% (Figure 5F), respectively. These results suggest that the markedly high levels of S-MBP protein after I/R operation might be explained by the influx of S-MBP from the circulation.

Discussion

Recent studies using MBP (S- and L-MBP) double KO mice (Møller-Kristensen et al. 2005) indicated that the complement activation through the MBP lectin pathway plays a critical role in the pathogenesis of ischemic acute renal failure. However, molecular mechanisms of this observation remain unclear. Particularly interesting is the identification of the ligand molecule associated with the initiation of the MBP lectin pathway. We previously identified metalloproteases meprins as endogenous MBP ligands, which are highly expressed in the brush border membranes of kidney proximal tubules (Hirano et al. 2005). However, it was not clear that MBP really interacts with meprins in vivo. Then, we try to clarify this point by focusing on the complement activation through the lectin pathway, which is known to be a major physiological function of MBP.

In the present study, we prepared renal I/R-operated mice as a model of acute renal failure. The immunohistochemical analyses of meprins, MBPs and complement component C3b, which is an activated form of C3, in the I/R-operated mouse kidney revealed marked changes in the distributions of these proteins, and co-localization of meprins with both S-MBP and C3b mainly on the base of the brush border on the proximal tubules. These results suggested the interaction of S-MBP with meprins occurred in the I/R-operated mouse kidney. Co-IP of meprins and S-MBP after chemical cross-linking demonstrated the formation of complexes of meprins and S-MBP, confirming the physical interaction of S-MBP with meprins in vivo, although the formation of cross-linked complexes is not so extensive due probably to a low accessibility of the cross-linking reagent to the site of complex formation on the surface of the cells, since small blocks of kidney tissue were treated with the reagent. Furthermore, in situ PLA (Söderberg et al. 2006) revealed explicitly in situ proximity of S-MBP with meprins on the base of the brush border of the proximal tubules in the I/R-operated mouse kidney. Moreover, the in vitro assay for complement activation demonstrated clearly that the interaction of S-MBP with meprins activated complement more remarkably than that with IgM Fc, which has high-mannose-type *N*-glycans recognized by MBP and is known to be a target of MBP on mesenteric I/R (Zhang et al. 2006). These lines of evidence obtained in this study indicate that S-MBP actually interacts with meprins in situ and that the interaction results in the pathological manifestations by activating complement through the lectin pathway. Bylander et al. (2008) reported that meprin β deficiency prevents renal I/R injury. In meprin β KO mice, secreting-type meprin α is not retained on the brush border membranes of the kidney

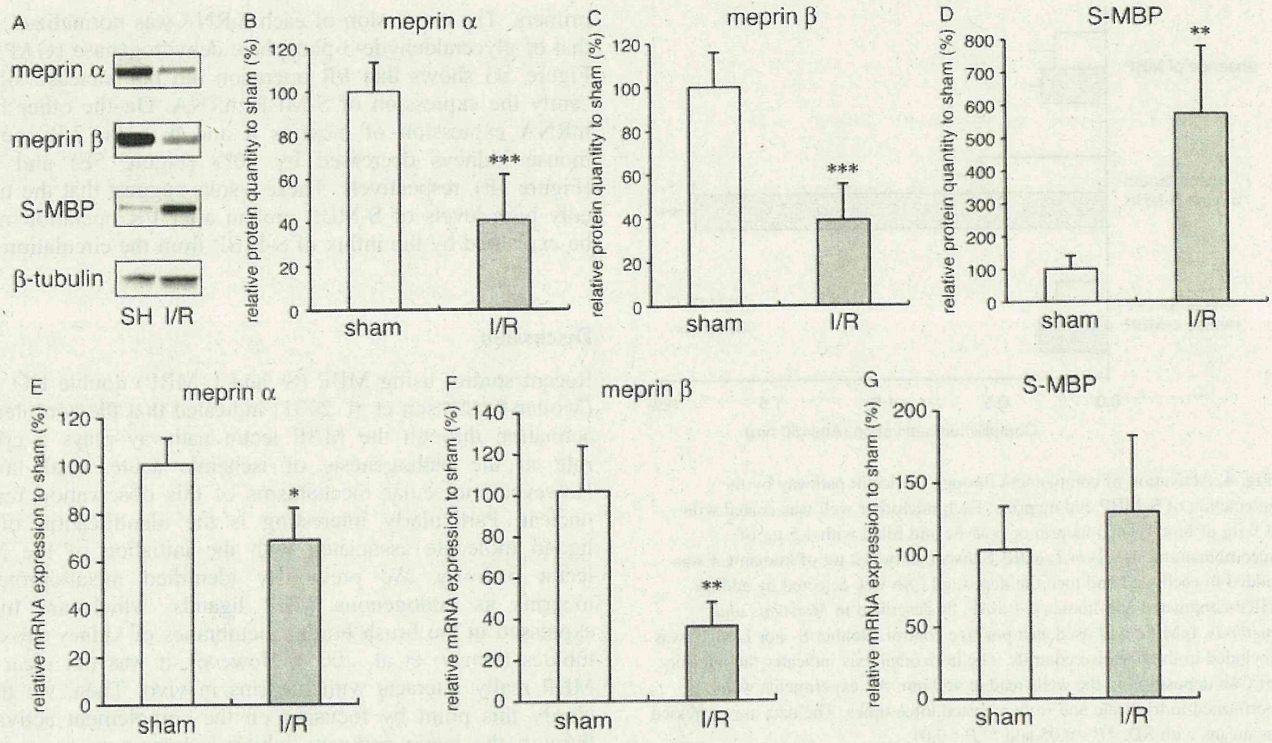

Fig. 5. Protein determination and mRNA levels of meprin α, meprin β and S-MBP in the I/R-operated mouse kidneys. (**A**) Western blotting analysis of meprins and S-MBP. SDS extracts of the renal cortex proteins of an I/R- and a sham (SH)-operated mouse were resolved on a 5–20% Tris–HCl gradient gel, and proteins, meprin α, meprin β, S-MBP and β-tubulin were detected by western blot analysis with their respective antibodies as described in *Materials and methods*. Relative protein levels of meprin α (**B**), meprin β (**C**) and S-MBP (**D**) were quantified as their band densities on western blotting analysis. Protein quantities were normalized as to the band density of β-tubulin. The data are expressed as means with SD ($n = 6$). (**E**–**G**) Total RNA was extracted from I/R- and sham-operated mouse kidney cortexes and subsequently reverse-transcribed with random hexamers. Real-time PCRs were performed with the resultant cDNA as a template, as described in *Materials and methods*. The mRNA expression of each was normalized as to the expression of GAPDH. The data are expressed as means with SD ($n = 6$). $^{*}P < 0.05$, $^{**}P < 0.005$ and $^{***}P < 0.001$.

proximal tubules and, therefore, it is reasonable to suppose that S-MBP can neither bind to the brush border membranes of the proximal tubules nor initiate complement activation.

Renal I/R operation significantly decreased the amounts of meprin proteins in the kidneys, whereas it increased the protein level of S-MBP, this being in complete agreement with the results of immunohistochemical analysis. Some years ago, we reported that S-MBP mRNA is expressed in the rat kidney (Morio et al. 1997). Then, we examined whether renal I/R increases the expression of S-MBP mRNA in the kidneys or not. The results of real-time PCR did not show significant changes of S-MBP mRNA expression in the I/R-operated mouse kidney. It was noted that the expression of S-MBP mRNA was slightly higher than that in the sham-operated kidney, suggesting the possibility that up-regulation of S-MBP mRNA expression may play some roles in this acute renal failure. This would be particularly so if the significantly down-regulated levels of meprins in the I/R-operated mouse kidney are taken into account. However, the markedly high level of S-MBP protein after the I/R operation may be explained most probably by the influx of S-MBP from the circulation. Although the glomerulus cannot filter out proteins that weigh >200 kDa (Tang et al. 2002) under the physiological condition, in the renal I/R-operated mouse kidney, this mechanism may not work properly.

Hemorrhagic shock or renal transplantation can lead to ischemic acute renal failure (Bonventre and Weinberg 2003). When the kidneys undergo ischemia, originally, the hypoxia damages the epithelial cells of the proximal tubules (Donohoe et al. 1978; Goligorsky et al. 1993). Additionally, the epithelial cells lose their polarity, and subsequently proteases that are normally localized on the apical surface of the epithelial cells are expressed on the basolateral membranes, where they degrade some extracellular matrix proteins (Kaushal et al. 1994; Fanning et al. 1999; Molitoris and Marrs 1999). This attenuates cell–cell or cell–matrix adhesion (Zuk et al. 1998). On the other hand, in the blood circulation of the kidney, some inflammatory mediators or cytokines, which are secreted by leukocytes activated by inflammation, facilitate vascular permeability (Bonventre and Zuk 2004). During this process, S-MBP can translocated to the proximal tubules from the blood circulation, interact with meprins on the brush border membranes of the proximal tubules, and then initiate the complement activation that results in necrosis of the tubular epithelial cells.

In conclusion, we demonstrate that S-MBP most probably derived from the blood circulation interacts with its endogenous ligands meprins in vivo in the I/R-operated mouse kidney and that the interaction initiates the complement activation through the MBP lectin pathway. These findings may contribute to the prevention of acute renal failure after renal transplantation, for example, by adding mannose as an inhibitor of the interaction of MBP with meprins to the preservation solution for the donor kidneys.

Materials and methods

Preparation of experimental renal I/R model mice

Six-week-old male BALB/c mice weighing 20–25 g were obtained from Japan SLC Inc. (Shizuoka, Japan) and were allowed free access to food and water during the experiments. The studies were carried out according to a protocol approved by the Institutional Animal Care Committee of Kyoto University. The experimental renal I/R model mice were prepared as described (Trachtman et al. 1995). In brief, mice were anesthetized with 45 mg/kg of sodium pentobarbital (Dainippon Sumitomo Pharma, Osaka, Japan). The body temperature was maintained at 37°C with a hot plate until the mice recovered from the anesthesia. An abdominal incision was made and ischemia was induced by bilateral renal artery clamping for 40 min. After removing the clamps, the wound was stitched up. The mice were sacrificed and their kidneys were removed for immunohistochemical analysis, protein quantification and real-time PCR at the indicated time points after ischemia. Sham-operated mice underwent the above-mentioned processes without renal artery clamping. During the operation, blood was sampled from the tail before ischemia, and 0, 1, 3, 6, 12 and 24 h after ischemia to quantitate BUN as an index of the severity of the acute renal failure using Urea N B (Wako, Osaka, Japan).

Immunohistochemical analysis

The I/R- and sham-operated kidneys were removed from mice that had been perfused with phosphate-buffered saline (PBS) and subsequently with PBS containing 4% (w/v) paraformaldehyde (PFA). The kidneys were fixed with 4% PFA/PBS overnight, dehydrated and then embedded in paraffin. Blocks were sectioned with a microtome (RM 2155; Leica, Wetzlar, Germany) at 10 μm and mounted on Matsunami adhesive silane-coated slides (Matsunami Glass Ind., Ltd, Osaka, Japan). Paraffin-embedded sections were deparaffinized with xylene and then hydrated with ethanol and PBS. Sections underwent microwave-stimulated antigen retrieval in 10 mM citrate buffer (pH 6.0) containing 1 mM ethylenediaminetetraacetic acid (EDTA) and then were rinsed with Tris-buffered saline (TBS) for 30 min. After blocking with horse serum (Vector Laboratories, Inc., Burlingame, CA), sections were incubated with 2.0 μg/mL goat anti-human meprin α or β polyclonal antibodies (R&D Systems, Minneapolis, MN) in TBS for 20 min at room temperature. Sections were washed in three changes of TBS containing 0.05% (v/v) Tween 20 (TBST) and then incubated with 1.0 μg/mL Alexa Fluor 546-labeled donkey anti-goat IgG (Invitrogen, Carlsbad, CA) in TBS for 30 min at room temperature. After washing in three changes of TBST, for double-immunofluorescence staining, sections were reacted with 10 μg/mL rat anti-mouse S-MBP mAb (8G6; Hycult Biotechnology, Uden, the Netherlands), 5 μg/mL rat anti-mouse L-MBP mAb (272801; R&D Systems) or 10 μg/mL rat anti-mouse C3b mAb (11H9; Abcam, Cambridge, MA) in TBS for 30 min at room temperature. Sections were washed in three changes of TBST and then incubated with 1.0 μg/mL Alexa Fluor 488-labeled rabbit anti-rat IgG (Invitrogen) in TBS for 30 min at room temperature. After washing in three changes of TBST again, sections were cover-slipped with Aqueous Mounting Medium PERMAFLUOR™ (Beckman Coulter, Marseille, France). Negative controls underwent staining with no primary antibodies. Fluorescent images were obtained under a confocal microscope, FluoView™ FV1000 (Olympus, Tokyo, Japan).

Chemical cross-linking, IP and immunoblotting

The I/R- and sham-operated kidneys were dissected from mice that had been perfused with PBS. Kidney cortexes were cut into small pieces. After washing three times with 0.1 M 2-[4-(2-hydroxyethyl)-1-piperazinyl]ethanesulfonic acid (HEPES, pH 7.4), pieces (40 mg) were subjected to cross-linking with 10 mM DSP (PIERCE, Rockford, IL) in 0.1 M HEPES (pH 7.4) for 30 min at room temperature, the reaction being stopped by adding 50 mM Tris–HCl (pH 7.5) to the reaction mixture followed by incubation for an additional 15 min at room temperature. Pieces were then washed three times with the homogenization buffer [150 mM NaCl, 20 mM Tris–HCl (pH 7.5), 1 mM EDTA and protease inhibitor cocktail (Nacalai Tesque, Kyoto, Japan)] and homogenized with a POLYTRON® (CH-6010; Kinematica, Luzernerstrasse, Switzerland) in 360 μL of the homogenization buffer. Homogenates were centrifuged (1000 × g, 10 min, 4°C) to remove cell debris and nuclei. Supernatants were solubilized with 1% (v/v) NP-40 and then centrifuged (105,000 × g, 1 h, 4°C). NP-40 lysates were incubated with 1 μg/mL goat anti-human meprin α (R&D Systems), 0.5 μg/mL goat anti-human meprin β polyclonal antibodies (R&D Systems) or 5 μg/mL anti-S-MBP mAb (8G6; Hycult Biotechnology), and complexes were precipitated with Protein G Sepharose 4B (GE Healthcare UK Ltd, Buckinghamshire, UK). Proteins bound to the beads were eluted with the SDS–PAGE sample buffer, resolved on a 5–20% Tris–HCl polyacrylamide gradient gel (ATTO, Tokyo, Japan) under non-reducing conditions and transferred to nitrocellulose membranes (Bio-Rad, Hercules, CA). Membranes were probed with anti-meprin α (R&D Systems), meprin β (R&D Systems) and anti-S-MBP antibody (8G6; Hycult Biotechnology), which recognizes only non-reduced forms of S-MBP, followed by HRP-conjugated respective secondary antibodies (Zymed, South San Francisco, CA) and developed by an enhanced chemiluminescence method (SuperSignal West Pico Chemiluminescent Substrate; PIERCE). Bands were visualized with a luminescent image analyzer, LAS-4000 mini (Fujifilm, Tokyo, Japan) and analyzed with standard image analysis software, MultiGauge ver. 3.0 (Fujifilm).

Detection of endogenous protein complexes in situ by proximity ligation

To investigate the in situ interaction between S-MBP and meprins, we performed the in situ PLA of paraffin sections of the I/R- and sham-operated mouse kidneys using Duolink™ in situ PLA (Olink Bioscience, Uppsala, Sweden) according to the manufacturer's instructions. In brief, sections, which had been deparaffinized, undergone microwave-stimulated antigen retrieval and blocked with horse serum (Vector Laboratories, Inc.), were incubated with 10 μg/mL rat anti-mouse S-MBP mAb (8G6; Hycult Biotechnology) and 2.0 μg/mL goat anti-human meprin α or β polyclonal antibodies (R&D Systems). After washing sections, they were reacted with the secondary antibodies conjugated with oligonucleotides (PLA probe MINUS for anti-S-MBP and PLA probe PLUS for anti-meprin α or β) for 2 h at 37°C. After washing sections with TBST, the two nucleotides were added to the hybridization buffer, followed by incubation for 15 min at 37°C to hybridize the two probes. Then the slides were washed with TBST and then reacted with ligase (1 U/section) for 15 min at 37°C to join the two hybridized oligonucleotides to close the circle when the PLA probes were in close proximity. A rolling-circle amplification (RCA) reaction that involves the formed circular oligonucleotide as a template was performed on sections for 90 min at 37°C by adding the nucleotides and polymerase (5 U/section) to generate a repeated sequence product extending from the oligonucleotide arm of the PLA probe. To detect the RCA product, Tex613 fluorophore-labeled oligonucleotide probes were hybridized to the RCA product for 60 min at 37°C. After washing with saline-sodium citrate buffer and 70% (v/v) ethanol, sections were cover-slipped with Aqueous Mounting Medium PERMAFLUOR™ (Beckman Coulter). Negative controls underwent staining with either anti-S-MBP or anti-meprin antibodies or with no primary antibodies. Fluorescent images were obtained under a confocal microscope, FluoView™ FV1000 (Olympus).

Purification of MBP from human serum, isolation of meprins from the mouse kidneys and preparation of biotin-labeled mouse meprins and human IgM Fc

Human MBP was purified from combined Cohn's fractions II and III, which had been prepared from healthy donors at Mitsubishi Pharma Co. (Osaka, Japan), by affinity chromatography on a mannan-agarose (Sigma-Aldrich, St Louis, MO) column, followed by a heparin-agarose (Tosoh, Tokyo, Japan) column as described previously (Nakamura et al. 2009). For the preparation of a Sepharose 4B-MBP column, human MBP was coupled to cyanogen bromide-activated Sepharose 4B (GE Healthcare UK Ltd), according to the manufacturer's instructions. Meprins were isolated from kidney membrane proteins with a Sepharose 4B-MBP column as described previously (Hirano et al. 2005). The isolated meprins and human IgM (Jackson ImmunoResearch Laboratories, Inc., West Grove, PA) were biotinylated with a FluoReporter Mini-Biotin-XX Protein Labeling Kit (Invitrogen) according to the manufacturer's instructions. The biotinylated proteins were used for the assay of the MBP lectin pathway.

Assay of complement activity through the MBP lectin pathway in vitro

The MBP lectin pathway was assayed essentially as described previously (Gadjeva et al. 2003). In brief, the microtiter wells of BD BioCoat™ Streptavidin Assay Plates (BD Biosciences, Bedford, MA) were coated with 1.0 μg aliquots of biotinylated meprins or IgM Fc in 100 μL of the coating buffer for 1 h at room temperature. Residual protein binding sites were blocked with 0.1% (w/v) human serum albumin in TBS for 1 h. After washing with TBST containing 10 mM $CaCl_2$ (TBST/Ca^{2+}), wells were filled with 100 μL of the MBP binding buffer with or without 1.5 μg of recombinant mouse S- or L-MBP (R&D Systems) at room temperature for 1.5 h. After washing with TBST/Ca^{2+} thoroughly, diluted MBP-deficient human serum was added to the wells to supply MASPs, followed by incubation overnight at 4°C. At the end of the incubation, 100 μL of 2 μg/mL human C4 (Sigma-Aldrich) diluted in C4 dilution buffer was added to each well, followed by incubation at 37°C for 1.5 h. Wells were washed with TBST/Ca^{2+}, and then the deposited C4b was detected by adding HRP-conjugated anti-human C4 mAb (Santa Cruz Biotechnology, Inc., Santa Cruz, CA) in TBST/Ca^{2+} at room temperature for 1 h. HRP activity was determined by adding 100 μL of the 3,3′,5,5′-tetramethylbenzidine liquid substrate system for ELISA (Sigma-Aldrich) to each well, and then plates were analyzed with a Multilabel Counter (PerkinElmer, Waltham, MA) at 450 nm. All experiments were performed in triplicate and were repeated three times.

Protein determination

The I/R- and sham-operated kidneys were dissected from mice that had been perfused with PBS. The kidney cortexes were cut into pieces weighing 50 mg and homogenized with POLYTRON® (CH-6010; Kinematica) in 450 μL of the homogenization buffer. Homogenates were centrifuged (1000 × *g*, 10 min, 4°C) to remove cell debris and nuclei. To each supernatant, one-fourth volume of 5× SDS–PAGE sample buffer [0.5 M Tris–HCl (pH6.8), 10% (w/v) SDS, 50% (v/v) glycerol and 0.005% (w/v) bromophenol blue with or without 25% (v/v) 2-mercaptethanol] was added and then the mixture was centrifuged (10,000 × *g*, 10 min, 4°C). Supernatants were resolved on a 5–20% Tris–HCl polyacrylamide gradient gel (ATTO), followed by transfer to nitrocellulose membranes (Bio-Rad). Membranes were incubated with 0.2 μg/mL goat anti-human meprin α polyclonal antibody (R&D Systems), 0.1 μg/mL goat anti-human meprin β polyclonal antibody (R&D Systems), 5 μg/mL rat anti-mouse S-MBP mAb (8G6; Hycult Biotechnology), 2 μg/mL anti-mouse L-MBP (272801; R&D Systems) or 0.1 μg/mL mouse anti-β-tubulin mAb (JDR.3B8; Sigma-Aldrich). For visualization, SuperSignal West Pico Chemiluminescence Kit (PIERCE) was used with HRP-conjugated secondary antibodies (Zymed). The luminescent bands were scanned with a luminescent image analyzer, LAS-4000 mini (Fujifilm) and analyzed with standard image analysis software, ImageJ ver. 1.44i.

Real-time PCR for measurement of mRNA expression

The I/R- and sham-operated kidneys were dissected from mice that had been perfused with diethyl

pyrocarbonate-treated PBS. Total RNA was extracted from the kidney cortexes with an RNeasy® Micro Kit (QIAGEN GmbH, Hilden, Germany), treated with an RNase-free DNase set (QIAGEN GmbH) and subsequently reverse-transcribed with a SuperScript® First-Strand Synthesis System for RT–PCR (Invitrogen) using random hexamers as primers according to the manufacturer's instructions. The resultant cDNA was used as the template for real-time PCR with gene-specific primers (Hokkaido System Science, Hokkaido, Japan). The sequences of the primers were as follows: meprin α, 5′-AGA GAC ATC CCA GCA GAC AGA AG-3′ (forward primer) and 5′-CCA TTC CCT TTA CGT TCA CAG A-3′ (reverse primer); meprin β, 5′-CGG CAT CAG CCT TGG TTT-3′ (forward primer) and 5′-TGT CTT GGT CAA TTC CTC CAT CT-3′ (reverse primer); S-MBP, 5′-GAA GGG AGA ACC AGG TCA AGG GC-3′ (forward primer) and 5′-CAT TGA GAA GGC ATG CAA CTT GTT-3′ (reverse primer); and GAPDH, 5′-GGA GAA ACC TGC CAA GTA TGA TG-3′ (forward primer) and 5′-TGG AAG AGT GGG AGT TGC TGT-3′ (reverse primer). Real-time PCRs were performed with ABI Prism® 7000 (Applied Biosystems, Lincoln Centre Drive Foster City, CA) in the presence of 30 μM each primer and 25 μL of FastStart Universal SYBR Green Master Mix (ROX) (Roche, Basel, Switzerland) in a total volume of 50 μL. The following PCR conditions were used for all samples: 95°C for 10 min, and then 37 cycles of 95°C for 15 s and 60°C for 30 s. The fluorescence intensity was monitored at the end of each amplification step. At the end of the reactions, the melting curves and quantities were analyzed with Sequence Detection System Software ver. 1.0 (Applied Biosystems).

Statistical analysis

Data are expressed as the means with SD and statistical analysis was performed with Microsoft® Excel 2004 for Mac® (Microsoft, Redmond, WA) by means of Student's *t*-test. $P < 0.05$ was taken to denote statistical significance.

Funding

This work was supported by Grant-in-Aid for Scientific Research on Priority Areas (14082203 to T.K.) from the Ministry of Education, Culture, Sports, Science and Technology of Japan; Grants-in-Aid for Scientific Research (C-20590074 to N.K. and B-18370057 to T.K.), Core-to-Core Program-Strategic Research Networks (17005), from the Japan Society for the Promotion of Sciences.

Acknowledgements

The authors thank Masaomi Nangaku, M.D., Ph.D. (Division of Nephrology and Endocrinology, University of Tokyo School of Medicine), for the helpful discussions and critical comments; Mr. Masahiro Hirata (Department of Diagnostic Pathology, Kyoto University Hospital) for the guidance in the preparation of paraffin sections; Mikio Nishizawa, M.D., Ph.D. (Department of Bioscience and Biotechnology, Ritsumeikan University), for the technical advice regarding real-time PCR; and Ms. Tomoko Tominaga for the secretarial assistance.

Conflict of interest

None declared.

Abbreviations

BUN, blood urea nitrogen; DSP, dithiobis(succinimidylpropionate); EDTA, ethylenediaminetetraacetic acid; ELISA, enzyme-linked immunosorbent assay; GAPDH, glyceraldehyde-3-phosphate dehydrogenase; HEPES, 2-[4-(2-hydroxyethyl)-1-piperazinyl]ethanesulfonic acid; HRP, horseradish peroxidase; Ig, immunoglobulin; IP, immunoprecipitation; I/R, ischemia/reperfusion; L-MBP, liver-type MBP; mAb, monoclonal antibody; MASP, MBP-associated serine protease; MBL, mannan-binding lectin; MBP, mannan-binding protein; mRNA, messenger RNA; NP-40, Nonidet P-40; PAGE, polyacrylamide gel electrophoresis; PBS, phosphate-buffered saline; PCR, polymerase chain reaction; PFA, paraformaldehyde; PLA, proximity ligation assay; RCA, rolling-circle amplification; SDS, sodium dodecyl sulfate; S-MBP, serum-type MBP; TBS, Tris-buffered saline; TBST, TBS with Tween 20.

References

Bond JS, Beynon RJ. 1986. Meprin: A membrane-bound metalloendopeptidase. *Curr Top Cell Regul.* 28:263–290.

Bonventre JV, Weinberg JM. 2003. Recent advances in the pathophysiology of ischemic acute renal failure. *J Am Soc Nephrol.* 14:2199–2210.

Bonventre JV, Zuk A. 2004. Ischemic acute renal failure: An inflammatory disease? *Kidney Int.* 66:480–485.

Bylander J, Li Q, Ramesh G, Zhang B, Reeves WB, Bond JS. 2008. Targeted disruption of the meprin metalloproteinase beta gene protects against renal ischemia-reperfusion injury in mice. *Am J Physiol Renal Physiol.* 294: F480–F490.

de Vries B, Walter SJ, Peutz-Kootstra CJ, Wolfs TG, van Heurn LW, Buurman WA. 2004. The mannose-binding lectin pathway is involved in complement activation in the course of renal ischemia-reperfusion injury. *Am J Pathol.* 165:1677–1688.

Donohoe JF, Venkatachalam MA, Bernard DB, Levinsky NG. 1978. Tubular leakage and obstruction after renal ischemia: Structural-functional correlations. *Kidney Int.* 13:208–222.

Fanning AS, Mitic LL, Anderson JM. 1999. Transmembrane proteins in the tight junction barrier. *J Am Soc Nephrol.* 10:1337–1345.

Gadjeva M, Thiel S, Jensenius JC. 2003. Assays for the mannan-binding lectin pathway. *Curr Prot Immunol.* 13.6:1–8.

Goligorsky MS, Lieberthal W, Racusen L, Simon EE. 1993. Integrin receptors in renal tubular epithelium: New insights into pathophysiology of acute renal failure [editorial]. *Am J Physiol.* 264:F1–F8.

Gorbea CM, Flannery AV, Bond JS. 1991. Homo- and heterotetrameric forms of the membrane-bound metalloendopeptidases meprin A and B. *Arch Biochem Biophys.* 290:549–553.

Gorbea CM, Marchand P, Jiang W, Copeland NG, Gilbert DJ, Jenkins NA, Bond JS. 1993. Cloning, expression, and chromosomal localization of the mouse meprin beta subunit. *J Biol Chem.* 268:21035–21043.

Hansen S, Thiel S, Willis A, Holmskov U, Jensenius JC. 2000. Purification and characterization of two mannan-binding lectins from mouse serum. *J Immunol.* 164:2610–2618.

Hirano M, Ma BY, Kawasaki N, Okimura K, Baba M, Nakagawa T, Miwa K, Kawasaki N, Oka S, Kawasaki T. 2005. Mannan-binding protein blocks the activation of metalloproteases meprin α and β. *J Immunol.* 175:3177–3185.

Ishmael FT, Noreum MT, Benkovic SJ, Bond JS. 2001. Multimeric structure of the secreted meprin A metalloproteinase and characterization of the functional protomer. *J Biol Chem.* 276:23207–23211.

Kaushal GP, Walker PD, Shah SV. 1994. An old enzyme with a new function: Purification and characterization of a distinct matrix-degrading metalloproteinase in rat kidney cortex and its identification as meprin. *J Cell Biol.* 126:1319–1327.

Liu H, Jensen L, Hansen S, Petersen SV, Takahashi K, Ezekowitz AB, Hansen FD, Jensenius JC, Theil S. 2001. Characterization and quantification of mouse mannan-binding lectins (MBL-A and MBL-C) and study of acute phase responses. *Scand J Immunol*. 53:489–497.

Marchand P, Tang J, Bond JS. 1994. Membrane association and oligomeric organization of the alpha and beta subunits of mouse meprin A. *J Biol Chem*. 269:15388–15393.

Molitoris BA, Marrs J. 1999. The role of cell adhesion molecules in ischemic acute renal failure. *Am J Med*. 106:583–592.

Møller-Kristensen M, Wang W, Ruseva M, Thiel S, Nielsen S, Takahashi K, Shi L, Ezekowitz A, Jensenius JC, Gadjeva M. 2005. Mannan-binding lectin recognizes structures on ischemic reperfused mouse kidneys and is implicated in tissue injury. *Scand J Immunol*. 61:426–434.

Morio H, Kurata H, Katsuyama R, Oka S, Kozutsumi Y, Kawasaki T. 1997. Renal expression of serum-type mannan-binding protein in rat. *Eur J Biochem*. 243:770–774.

Nakamura N, Nonaka M, Ma BY, Matsumoto S, Kawasaki N, Asano S, Kawasaki T. 2009. Characterization of the interaction between serum mannan-binding protein and nucleic acid ligands. *J Leukoc Biol*. 86:737–748.

Park P, Haas M, Cunningham PN, Bao L, Alexander JJ, Quigg RJ. 2002. Injury in renal ischemia-reperfusion is independent from immunoglobulins and T lymphocytes. *Am J Physiol*. 282:F352–F357.

Phaneuf LR, Lillie BN, Hayes MA, Turner PV. 2007. Binding of mouse mannan-binding lectins to different bacterial pathogens of mice. *Vet Immunol Immunopathol*. 118:129–133.

Söderberg O, Gullberg M, Jarvius M, Ridderstråle K, Leuchowius KJ, Jarvius J, Wester K, Hydbring P, Bahram F, Larsson LG, et al. 2006. Direct observation of individual endogenous protein complexes *in situ* by proximity ligation. *Nat Methods*. 3:995–1000.

Tang S, Lai KN, Sacks SH. 2002. Role of complement in tubulointerstitial injury from proteinuria. *Kidney Blood Press Res*. 25:120–126.

Thadhani R, Pascual M, Bonventre JV. 1996. Acute renal failure. *N Engl J Med*. 334:1448–1460.

Trachtman H, Valderrama E, Dietrich JM, Bond JS. 1995. The role of meprin A in the pathogenesis of acute renal failure. *Biochem Biophys Res Commun*. 208:498–505.

Wagner S, Lynch NJ, Walter W, Schwaeble WJ, Loos M. 2003. Differential expression of the murine mannose-binding lectins A and C in lymphoid and nonlymphoid organs and tissues. *J Immunol*. 170:1462–1465.

Zhang M, Takahashi K, Alicot EM, Vorup-Jensen T, Kessler B, Thiel S, Jensenius JC, Ezekowitz RA, Moore FD, Carroll MC. 2006. Activation of the lectin pathway by natural IgM in a model of ischemia/reperfusion injury. *J Immunol*. 177:4727–4734.

Zuk A, Bonventre JV, Brown D, Martin KS. 1998. Polality, integrin and extracellular matrix dynamics in the post-ischemic rat kidney. *Am J Physiol Cell Physiol*. 275:C711–C731.